

Contrails

WADC TECHNICAL REPORT 54-616

PART III

ASTIA DOCUMENT No. AD 110439

HYDROGEN CONTAMINATION IN TITANIUM AND TITANIUM ALLOYS

**Part III. Strain Aging Hydrogen Embrittlement
In Alpha-Beta Titanium Alloys**

HARRIS M. BURTE

MATERIALS LABORATORY

OCTOBER 1956

PROJECT No. 7851

**WRIGHT AIR DEVELOPMENT CENTER
AIR RESEARCH AND DEVELOPMENT COMMAND
UNITED STATES AIR FORCE
WRIGHT-PATTERSON AIR FORCE BASE, OHIO**

Carpenter Litho & Prtg. Co., Springfield, O.
600 - November 1956

Approved for Public Release

Contrails

FOREWORD

This report was prepared by the Metals Branch and was initiated under Project No. 7351, "Metallic Materials," Task No. 73510 "Titanium Metal and Alloys" and was administered under the direction of the Materials Laboratory, Directorate of Research, Wright Air Development Center, with Harris M. Burte acting as project engineer.

This report covers work conducted from July 1954 to October 1955.

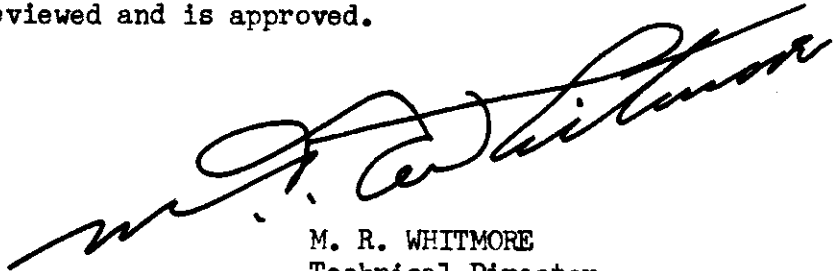
It is now well recognized that hydrogen contamination in alpha-beta titanium alloys can lead to sudden, brittle fracture during the use of these materials. The strain aging embrittlement which causes such fracture has been investigated.

Strain aging hydrogen embrittlement in alpha-beta titanium alloys has its greatest effect on mechanical properties measured at slow strain rates. It can cause low ductility in room temperature tensile tests and premature brittle fracture in room temperature rupture tests. Fracture due to this process tends to be intergranular. Metallographic examination of many hydrogen contaminated alpha-beta alloys shows no evidence for a third phase either before or after fracture. In at least one alloy, however, a third phase was visible after fracture. Both alloy composition and microstructure affect susceptibility to strain aging embrittlement. Increasing test temperature seems to decrease the tendency towards embrittlement, but increases the rate at which embrittlement can occur. A mechanism for strain aging embrittlement is proposed. Other types of embrittlement which may be caused by hydrogen are mentioned.

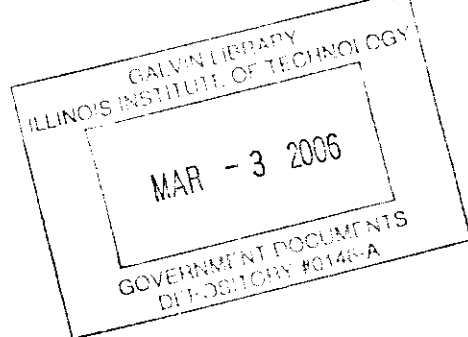
PUBLICATION REVIEW

This report has been reviewed and is approved.

FOR THE COMMANDER:



M. R. WHITMORE
Technical Director
Materials Laboratory
Directorate of Research



Contents
TABLE OF CONTENTS

<u>Section</u>	<u>Page</u>
I Introduction	1
II Experimental Methods	2
III Strain Aging Embrittlement	3
IV Specimen Surface Condition	4
V Specimen Type	5
VI Hydrogen Content	6
VII Heat Treatment and Alloy Composition	7
VIII Macroscopic Examination of Fractured Specimens	8
IX Microscopic Examination	9
X Discussion	10
XI Summary	12
XII Bibliography	14

Contrails
LIST OF ILLUSTRATIONS

<u>Figure</u>		<u>Page</u>
1	The Effects of Hydrogen on the Room Temperature Tensile Properties of Ti-140A, Ht. M1170. Unnotched Specimens Except Where Indicated.	25
2	The Effects of Hydrogen on the Room Temperature Rupture Behavior of Notched Specimens. In (A) the Height of a Line Extending Above a Point is Proportional to the Reduction in Area at Fracture.	26
3	The Influence of Time to Fracture on Ductility Measured in Room Temperature Tensile and Rupture Tests. Unnotched Specimens.	27
4	The Effects of Specimen Surface Condition	28
5	The Appearances of Fracture Surfaces for Unnotched Specimens	29
6	The Effects of Various Factors on Ductility Measured in Room Temperature Tensile Tests. Unnotched Specimens.	30
7	Mechanical Property Specimens that have been Tested. Not Drawn to Scale. Mechanical Property Data are Reported Only for the Unnotched and V-Notched Cylindrical Specimens.	31
8	Comparison of Room Temperature Data for Unnotched and V-Notched Cylindrical Specimens. C-130AM, Hydrogen = 320 ppm.	32
9	Photomicrographs of Ti-140A, Ht. M1192, 210 ppm Unstrained Material. Perpendicular to Rolling Direction. Mag. 500X.	33
10	The Appearances of Fractures in Notched Specimens of Ti-6Al-4V Sheet.	34
11	The Appearance of the Fracture Surface for Notched Specimens of High Hydrogen Material. Both Ends of One Specimen. Note the Post Fracture Cracks.	35
12	Post Fracture Cracking. Longitudinal Section Through Fractured End of Notched, High Hydrogen Specimen.	36
13	Photomicrographs of Ti-140A, Ht. M1170. Unstrained Material. Perpendicular to Rolling Direction. Mag. 500X	37
14	Photomicrographs of C-130AM, Ht. B3371. Perpendicular to Rolling Direction. Mag. 500X.	38

Contrails

LIST OF ILLUSTRATIONS (Continued)

<u>Figure</u>		<u>Page</u>
15	Photomicrograph of C-130AM, Ht. B5038, 320 ppm. Unstrained Material. Perpendicular to Rolling Direction. Mag. 500X. . . .	39
16	Photomicrographs of C-130AM, Ht. B5038, 320 ppm. Parallel to Rolling Direction. Mag. 500X.	40
17	Photomicrographs of Ti-150A, Ht. R68, 250 ppm. Perpendicular to Rolling Direction. Mag. 500X.	41
18	Photomicrographs of Ti-150A, Ht. R68, 250 ppm. Parallel to Rolling Direction. Mag. 500X.	42
19	Photomicrograph of Ti-155AX, 260 ppm. Unstrained Material. Perpendicular to Rolling Direction. Mag. 500X. This Material not Susceptible to Strain Aging Hydrogen Embrittlement.	43

Contrails

LIST OF TABLES

<u>Table</u>		<u>Page</u>
I	Analyses of Titanium Alloys	16
II	Preparatory Treatments to Adjust Hydrogen Content and Thermal History	17
III	The Effects of Hydrogen Contamination on the Room Temperature Tensile and Rupture Behavior of C-130AM, Ht. B5038. Unnotched Specimens	19
IV	The Effects of Hydrogen Contamination on the Room Temperature Rupture Behavior of Ti-140A, Ht. M1170. Unnotched Specimens	20
V	The Effects of Specimen Surface Condition on the Room Temperature Tensile Behavior of Low Hydrogen Material	21
VI	The Effects of Specimen Surface Condition on the Room Temperature Rupture Behavior of C-130AM, Ht. B5038.	22
VII	The Effect of Heat Treatment on Susceptibility to Hydrogen Embrittlement. Room Temperature Rupture Tests on Notched Specimens of Ti-140A, Ht. M1192	23
VIII	Room Temperature Mechanical Properties of a Material Which Does Not Exhibit Strain Aging Embrittlement at a Hydrogen Content of 260 ppm. Ti-155AX	24

Contrails

Contrails

I. INTRODUCTION

One of the important phases of research in titanium and titanium alloys has been concerned with the effects of interstitial contaminants on the properties of these materials. From the very first much attention was devoted to the effects of oxygen, nitrogen and carbon; recently the effects of hydrogen have been the subject of extensive research.

The early work of Jaffee and co-workers (1, 2, 3) on unalloyed titanium showed that hydrogen is relatively soluble in the beta, body centered cubic, elevated temperature phase of titanium, but at room temperature is quite insoluble in the alpha, hexagonal close packed, low temperature phase. In unalloyed titanium or alloys with low contents of alpha stabilizing elements, which at room temperature are predominantly alpha phase, hydrogen in excess of the solubility limit is precipitated as hydride needles or platelets, and this increases the classical ductile to brittle transition temperature. Thus the effects of hydrogen contamination on the ductility of these all-alpha materials is greatest at high strain rates, in the presence of a notch, and at low test temperatures. Hydrogen contamination in the range 0-500 parts per million by weight (ppm) has little effect on properties measured in normal room temperature tensile tests, but has a pronounced effect on the energy absorption measured in a notch-bend impact test.

In alloys with beta stabilizing elements such as iron or manganese, both alpha and beta phases may be present at room temperature, and the effects of hydrogen on mechanical properties are quite different from those for the all-alpha alloys (4, 5, 6, 7). These alpha-beta alloys are representative of many of the commercially available titanium alloys, and the remainder of this report is concerned with these two phase alloys. Jaffee et. al. (4, 7), and Kotfila and Erbin (5) showed that in several alpha-beta alloys hydrogen content does not cause a hydride precipitate but does induce a strain rate sensitivity leading to low ductility in tensile tests at slow testing speeds. This is exactly opposite from the effect of strain rate on the ductility of all-alpha alloys. It was suggested that in alpha-beta alloys hydrogen contributes to a strain aging type of embrittlement. The problem of the effects of hydrogen in alpha-beta titanium alloys assumed practical rather than academic importance during the spring of 1954 when failures in aircraft parts were reported that could be attributed to hydrogen embrittlement. Work at Pratt and Whitney Aircraft Corporation showed that hydrogen could cause premature brittle fracture under conditions of sustained loading. Other work on alpha-beta alloys has been reported (8, 9, 10). The results of an initial investigation at Materials Laboratory, Directorate of Research, Wright Air Development Center have been presented in Part 1 of this report (Reference 6). Part 2 dealt with methods of analysis for hydrogen. This Part 3 is concerned with the effects of hydrogen on the room temperature mechanical properties of alpha-beta titanium alloys, and the mechanism of strain aging hydrogen embrittlement.

Manuscript released by author October 1956 for publication as a WADC Technical Report.

II. EXPERIMENTAL METHODS

The materials for which mechanical property test data are reported are described in Table I. They are all commercial or semi-commercial alpha-beta alloys which were supplied in the form of barstock. Experiments were also performed on sheet material, and on specimens from forged articles, but since these gave results similar to those for barstock they will be discussed in a qualitative manner only. The preparatory procedures described in Table II were performed on the as-received stock in order to obtain different levels of hydrogen contamination in specimens from one heat of a given material. In order to isolate the effects of hydrogen contamination from those of other metallurgical variables, the materials of different hydrogen levels prepared from one heat were brought to similar thermal histories before test specimens were machined. Hydrogen content was decreased below that of as-received material by vacuum annealing; the pressure, measured in a room temperature zone in the vacuum annealing system was usually below 0.1 micron, and sometimes was as low as 0.01 micron. The hydrogen content was increased over that in the as-received material by heating in a hydrogen atmosphere. Thermal history adjustment and homogenization of hydrogen content across specimen cross-section were accomplished by heating in air or inert gas. No differences could be attributed to the use of air vs. an inert gas since the contaminated surface resulting from heating in air was removed during the machining of test specimens.

Hydrogen analyses were by the vacuum fusion method. Annealing in air or inert gas, or mechanical property testing had no discernable effect upon the hydrogen content. Hydrogen contents are expressed as parts per million by weight (ppm).

Room temperature mechanical property test data are reported for notched and unnotched cylindrical specimens machined from the barstock. Tensile tests were performed at various strain rates corresponding to the testing speeds indicated. Rupture (sustained loading) tests were performed on standard lever-arm creep-rupture frames. In many cases several specimens were loaded in tandem on a single frame. When one specimen broke a new one or a dummy was inserted, and the stress was reapplied. Room temperature for rupture testing was controlled between 72°F to 74°F; room temperature for tensile testing was not controlled and may have varied between 70°F to 90°F.

The unnotched cylindrical specimens had a gage length of 1 inch and a gage diameter of 0.137 inch. The notched cylindrical specimen was a 0.294 inch bar with a circumferential 60° V-notch that reduced the load-carrying area to a circle 0.137 inch diameter. Radius at root of notch was 0.01 inch. Specimen ends for both types were 3/8 inch diameter with 16 threads per inch. The majority of the unnotched specimens were tested with as-machined, or as-machined and rough polished surfaces. The effect of specimen surface preparation was also investigated.

Confidential

Metallographic specimens were mechanically polished and were etched with one of the following mixtures.

48%	HF	=	2% (by volume)	2%	20%
conc.	HNO ₃	=	10%	-	20%
	H ₂ O	=	88%	98%	-
glycerine		=	-	-	60%

III. STRAIN AGING EMBRITTLEMENT

Tensile and rupture test data for two titanium alloys are presented in Figures 1, 2a and 2c and Tables III, IV. Considering first the tensile test data; hydrogen content between 10 and 400 ppm has little effect on the ultimate tensile strength, the yield strength, or the ratio of notch strength to unnotch strength. Ductility, as measured by elongation or reduction in area is reduced by hydrogen content, but the amount of the reduction is not a single valued function of hydrogen content. It depends on the strain rate at which the test is performed and other factors which will be discussed below. At high strain rates hydrogen containing material may show the same ductility as hydrogen free material, whereas at low strain rates the ductility may be greatly reduced. This strain rate dependence of the tensile test ductility of hydrogen containing material is characteristic of the embrittlement under consideration, and suggests that it arises from some strain aging mechanism. Two important features of this strain aging embrittlement are how slow the strain rate must be for an appreciable ductility reduction to be apparent, and the minimum hydrogen content required to produce it at any strain rate.

Consider now the rupture test data for unnotched specimens. For both hydrogen free and hydrogen containing materials, as the stress level is decreased the time to fracture is increased. The rate of increase of fracture time with decrease of stress is much greater for hydrogen free than for hydrogen containing material. Furthermore, the ductility of hydrogen free specimens is relatively independent of stress level or time to fracture, whereas that of hydrogen containing specimens decreases markedly as time to fracture increases. Very high stress levels and short fracture times correspond to rapid rates of plastic deformation and this is analogous to fast strain rates in the tensile test. In Figure 3, ductility measured as reduction in area is plotted against time to fracture for both tensile test and rupture test specimens. It is recognized that such a comparison can be only approximately valid, but the data do indicate the importance of time to fracture in determining the extent of embrittlement developed in either tensile or rupture tests. Time to fracture in the tensile test is controlled by the strain rate, and in the rupture test by the stress level. If time to fracture is sufficiently short the hydrogen contaminated material tends to act in a ductile manner.

It was difficult to make accurate measurements of ductility for the notched specimens, however, the data that are presented in Figure 2a include an indication of the reduction in area at fracture. Qualitatively, the behavior of notched specimens is quite comparable to that of unnotched specimens. At very high stresses and short fracture times the hydrogen free and hydrogen containing specimens fracture in comparable times, both in a ductile manner. At lower stress levels where the hydrogen free specimens fracture in long times still in a ductile manner, or do not fracture, the hydrogen containing specimens exhibit premature brittle fracture. The data in Figure 2c are all in the range in which the hydrogen containing specimens fracture in a premature brittle manner.

In rupture tests as in tensile tests there are two important features of the strain aging embrittlement; a minimum rupture time which is necessary for embrittlement to be observed, and a minimum hydrogen content for premature brittle fracture even at very long rupture times. It is evident that a strain aging mechanism for the hydrogen embrittlement must explain premature and low stress fracture in sustained loading as well as the strain rate sensitivity of the ductility.

The characteristic qualitative features of the strain-aging hydrogen embrittlement are as is described above; the influence of factors such as specimen surface condition, specimen type, hydrogen content, alloy composition, and microstructure will be discussed below. All of these factors affect quantitative rather than qualitative aspects of the embrittlement.

IV. SPECIMEN SURFACE CONDITION

The unnotched cylindrical specimens that were tested had one of the following surface conditions: as-machined; machined + rough polish; machined + fine polished through 0000 metallographic paper. The appearances of the specimen surfaces are illustrated in Figure 4 which shows broken ends of mechanical property test specimens. For the as-machined specimens, the intersection of the fracture surface with the specimen surface coincides with machining marks around most if not all of the specimen circumference. For rough polished specimens part of the intersection of the fracture surface with the specimen surface coincides with polishing scratches. For the fine polished specimens there was no apparent influence of specimen surface marks. These observations are general for both hydrogen free or hydrogen containing specimens tested in tensile and rupture tests.

The appearances of the fracture surfaces of unnotched specimens are shown in Figure 5, and will be discussed more fully in section VIII. Two types of fracture surface are observed, one for specimens which fracture in a ductile manner, and one for specimens which fracture due to strain aging hydrogen embrittlement. For either ductile or hydrogen embrittled specimens, the appearance of the fracture surface is similar for all three types of specimen surface.

The ductile fracture specimens show a classical "cup and cone," and it is generally agreed that fracture is initiated in the interior of such a specimen. The effects of surface condition on tensile or rupture properties should be minor for specimens with this type of fracture. For the brittle fracture specimens with as-machined or rough polished surfaces, the fracture nucleus can usually be associated with a scratch on the surface. For the fine polished, brittle fracture specimens no association of the fracture nucleus with visible surface scratches is apparent.

Data on the effects of specimen surface condition on mechanical properties are presented in Table V and Figures 6d and 6e for tensile tests, and in Table VI for rupture tests. As expected, specimen surface condition has no significant effect upon the mechanical properties of ductile, hydrogen free material. For hydrogen containing material specimen surface condition does not affect qualitative features of the strain aging embrittlement, but it does have quantitative effects. In rupture tests at a given stress level, the polished specimens require a longer time for premature brittle fracture. In tensile tests there is an indication that polished specimens may require slower strain rates for an appreciable ductility reduction to be apparent. An alternate explanation of the tensile test data in Figures 6d and 6e is that in some alpha-beta alloys hydrogen can cause a notch sensitivity type of embrittlement at fast strain rates in addition to the strain aging embrittlement being considered here.

With the exception of the fine polished specimens of Ti-150A, and the specimens of Ti-140A, Ht. M1170, 250 ppm, the unnotched hydrogen containing (above 100 ppm) specimens for which data are reported in Tables III and IV and Figures 1, 3 and 6 have as-machined surfaces. The specimens of Ti-140A, Ht. M1170, 250 ppm had as-machined + rough polished surfaces.

Any conclusions in this report which rest upon quantitative aspects of the tensile or rupture data have been evaluated for the possibility that variations in specimen surface condition are producing spurious results. Quantitative comparisons are presented only when such a possibility is very remote.

The V-notched cylindrical specimens tested were all machined in the same way. Observation of fractured specimens indicates no evidence for any effects of machining marks at the root of the notch.

V. SPECIMEN TYPE

A variety of notched and unnotched tensile and rupture test specimens have been used (Figure 7). These have included cylindrical specimens from barstock and forgings and flat specimens from various gages of sheet. The effects of hydrogen on tensile and rupture test behavior are qualitatively the same for all of these specimen types.

Rupture data for unnotched and V-notched cylindrical specimens are compared in Figure 8. The extrapolation of the curve for notched specimens to cross that for unnotched specimens is justified by the general experience that these notched specimens can show premature brittle fracture at lower nominal stresses than unnotched specimens (e. g. see data for Ti-140A, Ht. M1170). Premature brittle fracture in notched specimens can occur at nominal stresses as low as 40% of the short time notched tensile strength. The qualitative features of strain aging hydrogen embrittlement are the same for both types of specimens. For each there is a stress above which fracture will be ductile due to short fracture time, and naturally there is a stress below which fracture will not occur in time periods of practical interest. In each case there is an intermediate range of stress over which hydrogen contaminated specimens fracture prematurely, in a brittle manner. However for this V-notched specimen, the range of stress (nominal stress based on original cross-sectional area) over which premature brittle fracture can occur is much greater than for unnotched specimens. Two factors must be considered to understand the effect of this type of notch: the triaxial stress state which tends to restrict plastic flow, and the stress concentration near the root of the notch. The former causes the short time notch tensile strength to be greater than the unnotched ultimate tensile strength. The latter allows long time premature brittle fracture to occur at lower stresses in notched than in unnotched specimens. As a result, for short rupture times the notched specimens require a higher stress than the unnotched specimens; for relatively long times to rupture the reverse is true.

VI. HYDROGEN CONTENT

At the low hydrogen contents of the vacuum annealed "hydrogen free" material none of the alloys tested exhibit any tendency towards strain aging embrittlement. There must therefore, be some minimum hydrogen content below which embrittlement will not occur no matter how slow the strain rate is in a tensile or rupture test.

The influence of hydrogen content above this minimum, on tensile test ductility, is illustrated by the data in Figure 6c and 6d. At a hydrogen content of 170 ppm the alloy Ti-140A, Ht. M1170 will show premature brittle fracture in rupture tests and it can therefore be assumed that there would be a reduction in tensile test ductility if slower strain rate tensile tests were performed. It may be concluded that increasing hydrogen content allows an increase in the strain rate which must be used for an appreciable ductility reduction to be apparent. The data in Figure 6d indicate that for a given strain rate the amount of the ductility reduction increases as the hydrogen content increases.

Since the dependence on strain rate or time to fracture is similar in tensile and rupture tests, increasing the hydrogen content must decrease the minimum time to fracture at which premature brittle fracture can be observed in a rupture test. The times to fracture for the data in Figures 6c and 6d are above this minimum, and the hydrogen containing specimens show premature brittle fracture. At a given stress level in this range of

Contrails

behavior, increasing the hydrogen content decreases the time required for premature brittle fracture.

VII. HEAT TREATMENT AND ALLOY COMPOSITION

Rupture test data on two heat treated conditions of a hydrogen containing material are presented in Table VII. One set of otherwise identical specimen blanks was furnace cooled from a temperature low in the alpha-beta range for this alloy, the other was air cooled from a temperature higher in the alpha-beta range. Microstructures obtained are shown in Figures 9a and 9b. The rupture data indicate that heat treatment alone can cause profound differences in the susceptibility of a given alloy to hydrogen embrittlement.

At appropriate hydrogen levels or heat treatments strain aging hydrogen embrittlement has been observed in alpha-beta alloys with the following nominal compositions:

Ti-8Mn	Ti-2Fe-2Cr-2Mo
Ti-4Al-4Mn	Ti-3Mn-1Fe-1V-1Cr-1Mo
Ti-6Al-4V	
Ti-1.5Fe-2.7Cr	

Note that embrittlement can occur whether or not a eutectoid reaction is possible.

As a consequence of the vacuum annealing, hydrogenation and homogenization treatments described in the Section II, the materials now to be discussed were in annealed low in the alpha-beta region + furnace cooled conditions. Microstructures before mechanical property testing are shown in Figures 13, 14b, 15, and 17a. Variations in prior mill processing caused a variety of microstructures even though the final thermal treatments for these materials were similar. Tensile and rupture data pertinent to this discussion are contained in Figures 2, 3 and 6 and Table VIII. It is evident that although heat treatment can have an effect, susceptibility to hydrogen embrittlement is not peculiar to one particular type of microstructure.

The tensile test data in Figures 6a and 6b are for two heats of nominally the same alloy, both given final thermal treatments of furnace cool from 1300°F, and both with very similar microstructures. Due to slight differences in composition or mill processing a much lower strain rate (longer time to fracture) must be used in order to observe embrittlement in Ht. B5038 than in Ht. B3371 even though the former has a higher hydrogen content. The notch rupture test data in Figures 2a and 2b show a similar difference in the time to rupture at a given stress level. Other comparisons are possible from the data in Figures 2, 3, and 6 to show that alloy composition or microstructure or an interaction between these two can affect quantitative features of the embrittlement such as minimum time to fracture for embrittlement to be produced in either tensile or rupture tests, or time to premature brittle fracture at a given stress level in the rupture test.

Contrails

For example, even polished specimens of Ti-150A, Ht. R68 at 250 ppm require a shorter minimum time to fracture in tensile tests than as-machined specimens of C-130AM, Ht. B5038 at 320 ppm.

Table VIII and Figure 18 present data for an alpha-beta alloy, in an annealed condition, at a hydrogen level which does cause embrittlement in many other alpha-beta alloys. However, this alpha-beta alloy does not show any evidence for strain aging hydrogen embrittlement. It is evident that composition or microstructure or an interaction between these two can also affect the minimum hydrogen content which can cause embrittlement even at very slow strain rates.

Although these data do not provide an unequivocal demonstration of the effect of composition as separated from the possible effects of heat treatment or an interaction between composition and heat treatment, it is felt that composition must be an important primary variable contributing to the susceptibility of a given material to strain aging hydrogen embrittlement.

VIII. MACROSCOPIC EXAMINATION OF FRACTURED SPECIMENS

The appearances of the fracture surfaces of unnotched cylindrical specimens are presented in Figure 5 and have been partially discussed. Ductile fracture, whether for hydrogen free material, or for hydrogen containing material tested at high strain rates, results in a characteristic "cup and cone" appearance around the entire circumference of the specimen. For brittle fracture the cup and cone characteristics are greatly reduced and do not extend entirely around the specimen circumference. The portion of the fracture surface which is perpendicular to the specimen axis has a relatively smooth area adjacent to the portion of the specimen circumference where the cup and cone appearance is absent, and a rougher area radially opposite to this. It should be mentioned that similar fracture surfaces have been observed to result from brittle behavior in titanium alloys due to causes other than strain aging hydrogen embrittlement.

The appearance of ductile, and premature brittle fractures in notched sheet specimens is presented in Figure 10. Premature brittle fractures contain a smooth area, perpendicular to the specimen axis, extending from the root of the notch. Note that the extent of this smooth area is greater, the smaller the stress level which caused fracture.

The appearance of these hydrogen embrittled fracture surfaces suggests that the nucleus of fracture is in the smooth area at or near the specimen surface. Premature brittle fracture consists of growth of this nucleus into a crack which propagates across the specimen until the residual cross-sectional area can no longer support the applied load, followed by ductile fracture in this residual cross-section.

Contrails

The appearance of the fracture surface of a hydrogen containing V-notched cylindrical specimen is shown in Figure 11. With these specimens it was not possible to establish clear-cut differences between the general appearances of ductile and premature brittle fractures, but it was noted that hydrogen contaminated specimens contain cracks running more or less parallel to the specimen axis. The intersection of such cracks with the fracture surface can be seen in Figure 11. A section taken parallel to the specimen axis is shown in Figure 12, and further illustrates the nature of these cracks. A few tensile test specimens were examined immediately after fracture and thereafter. In this case, visible cracks could not be detected immediately after fracture but were present 1 week later. Examination of all other specimens was at least several weeks after fracture. In general, the crack traces in the fracture surfaces of the two broken ends of the specimen do not coincide if the fracture surfaces are brought together; this is another indication that most of the cracks tend to form over a period of time after fracture. Such post fracture cracks are found in the broken ends of almost all cylindrical V-notched specimens where the hydrogen content is such as to render the particular material under test susceptible to strain aging embrittlement. They occur irrespective of whether high or low strain rates leading to ductile or brittle original fractures are used. Post fracture cracks are also prevalent in unnotched cylindrical specimens if high strain rates leading to ductile fractures preceded by necking are employed. Unnotched specimens which fail in a brittle manner, with little or no necking, exhibit little or no post fracture cracking.

It is evident that this post fracture cracking is due to the same strain aging hydrogen embrittlement that leads to premature brittle fracture in rupture tests, and is caused by residual radial stresses in the 2 halves of the fractured specimen. The radial stresses are set up by the triaxial stress state induced in cylindrical specimens by a notch or necked region.

IX. MICROSCOPIC EXAMINATION

Representative microstructures of unstrained material, and of material near the fracture surfaces of test specimens are shown in Figures 13 to 19. Sections have been taken both perpendicular to and parallel to the rolling direction of the barstock. The hydrogen free and hydrogen containing materials, in an unstrained condition, have essentially the same microstructure. Examination of the region near fracture in mechanical property test specimens shows that testing does not affect the microstructure of hydrogen free material. Similarly, for many of the materials tested, fracture due to strain aging hydrogen embrittlement is not accompanied by visible microstructural changes. There are occasionally some indications of a precipitate near the ends of post fracture cracks, but this evidence is not at all clear-cut. For Ti-150A, Ht. R68 a dark etching precipitate does appear in strained regions of the hydrogen containing fractured test specimens. It is most prevalent near the original fracture surface and around the ends of post fracture cracks. This precipitate can be redissolved to yield a microstructure comparable to that

Contrails

in unstrained material by heating in air or inert gas. Most of the precipitate disappears after 45 hours at 800°F; after 7 hours at 1200°F it has been completely redissolved. Figure 17d shows a partially redissolved precipitate at the end of a post fracture crack.

The post fracture cracks present in Figures 14c, 16b, 17c, and 18c tend to follow an intergranular path. From this it may be concluded that strain aging hydrogen embrittlement leads to intergranular fracture.

X. DISCUSSION

There is a marked similarity between the qualitative aspects of hydrogen embrittlement in steel (11, 12, 13, 14) and strain aging hydrogen embrittlement in alpha-beta titanium alloys. It is quite possible that the mechanisms of embrittlement are also very similar.

The following is proposed as the framework for a mechanism of strain aging hydrogen embrittlement in alpha-beta titanium alloys. Initially, in unstrained material, the hydrogen is in interstitial solid solution. Plastic deformation provides microscopic regions towards which there is a tendency for the hydrogen to segregate. The net result of such microsegregation is to provide regions, where microcracks can be initiated and propagate, thus providing a low stress route to brittle fracture.

The similarity between the microstructures of unstrained hydrogen free and hydrogen containing alpha-beta alloys suggests that initially the hydrogen is in interstitial solid solution. The titanium-hydrogen phase diagram (3) indicates that hydrogen is a beta phase stabilizer, and has very little room temperature solid solubility in unalloyed alpha phase. It is conceivable that alloying the alpha or beta phases can change the solid solubilities of hydrogen in these phases, but in alpha-beta alloys such as Ti-1.5Fe-2.5Cr in which the alpha phase is relatively pure, the hydrogen, at room temperature, is probably partitioned to the beta phase. Even within unstrained beta phase there will be a tendency for the interstitial hydrogen atoms to segregate to lattice defects such as dislocations, vacancies, or grain boundaries. The intercrystalline nature of hydrogen embrittlement fractures suggests that plastic deformation affects the structure in some manner as to establish more sites for such segregation at the grain boundaries. The hydrogen atoms will tend to diffuse towards such sites. The extent of such microsegregation will depend upon the extent of the deformation, the partition function between the new sites and the remainder of the beta phase, the initial concentration of hydrogen in the beta phase, and the rate at which the necessary diffusion can occur. It is suggested that if this microsegregation causes a high enough local concentration of hydrogen atoms, a microcrack can be formed. The exact manner of formation of the intercrystalline microcrack cannot yet be described; in at least one of the materials tested there is evidence that it involves formation of a third, possibly hydride phase. Another possibility involves condensation of molecular hydrogen in lattice vacancies. Growth of the microcrack may involve a continuation of this embrittlement process in the strained material around the periphery of the crack.

Application of this mechanism to the mechanical property data must consider both the tendency towards microsegregation and the rate at which microsegregation and consequent embrittlement can occur. The tendency towards microsegregation is provided by the initial hydrogen concentration, and plastic deformation which may be quite localized. The rate of microsegregation, involving diffusion of the hydrogen, may be relatively slow. Ductility measured in a tensile test will depend upon the rate at which this microsegregation can occur relative to the rate of straining imposed on the material. At high strain rates the material fails in a ductile manner by plastic deformation before appreciable microsegregation and consequent embrittlement can occur. At very slow strain rates a localized region of the specimen is sufficiently deformed to induce microsegregation, and this takes place with consequent fracture before total deformation of the specimen is very great. Similarly, in rupture tests at very high stress levels the rate of straining due to creep is so great that ductile fracture occurs before microsegregation is appreciable. At low stresses, where creep is slow, a critical amount of deformation in a localized section leads to microsegregation and fracture before much creep can occur. This can happen even at stress levels where the creep is so slow that normal ductile fracture would not occur in time periods of practical interest. The time for premature brittle fracture in a rupture test at a given stress level will depend upon the time required for sufficient plastic deformation to initiate the embrittlement, the rate at which microsegregation occurs, and the rate of propagation of the microcrack which is formed.

A stress-concentration such as exists at a notch or a surface scratch can lower the stress, or at a given stress can decrease the time required for sufficient localized plastic deformation to initiate the embrittlement. In some notched specimens the complicating influences of triaxial stress states must be considered.

At this stage in the discussion the information available (5, 6, 7, 9) on the effects of test temperature on strain aging hydrogen embrittlement should be considered. If tensile tests at a constant slow strain rate are performed over a range of temperatures the ductility reduction due to hydrogen is zero at high temperatures, goes through a maximum as temperature is decreased, and again approaches zero at very low temperatures. The temperature of the maximum ductility reduction depends upon the alloy, hydrogen content, and strain rate, and may be below room temperature. Rupture tests performed at room and elevated temperatures indicate that a hydrogen content that leads to premature brittle fracture at room temperature, may not do so at elevated temperatures. Rupture tests at subzero temperatures have not been reported.

These data suggest that temperature affects both the susceptibility towards embrittlement at a given hydrogen content, and the rate at which embrittlement can occur. Increasing test temperature might be expected to affect the tendency for hydrogen to partition between general interstitial solid solution and microsegregation to deformation induced sites in favor of the former. Therefore, increasing test temperature decreases

the tendency towards embrittlement. Decreasing the temperature decreases the rate at which hydrogen can diffuse, and therefore decreases the rate at which embrittlement can occur even though the tendency towards embrittlement is increased. In tensile tests at a constant strain rate there will be no ductility reduction at elevated temperatures because there is no tendency towards embrittlement. At very low temperatures there is no ductility reduction because the rate of embrittlement is slow with respect to the strain rate. Between these two temperature extremes the ductility reduction goes through a maximum.

The effects of composition and microstructure on susceptibility to strain aging hydrogen embrittlement have been demonstrated, and may be due to many causes. Composition can be expected to affect the solubilities of hydrogen in the alpha and beta phases, and the partition between general interstitial solution and microsegregation. Heat treatment can affect the ratio of alpha phase to beta phase present at room temperature, and the compositions of these phases. Heat treatment and differences in content of other interstitial elements can affect the nature of the alpha-beta grain interfaces, which, since fracture is intergranular, should influence the strain aging embrittlement.

Attention in this report has been focussed on strain-aging hydrogen embrittlement; it must be pointed out, however, that hydrogen can have additional effects on the properties of alpha-beta alloys. With some alpha-beta alloys a suitable combination of hydrogen content and heat treatment may result in material which, at room temperature, has a hydride phase in its microstructure (15). This might be expected to produce the greatest reduction in ductility when the material is tested at fast strain rates and in itself should not cause the premature brittle fracture in rupture tests which is characteristic of strain aging embrittlement. At elevated temperatures where strain aging embrittlement does not occur, a different type of embrittlement frequently takes place (6). Here, specimens which have been exposed to elevated temperature creep conditions are found to have lowered ductility when tested in subsequent room temperature, fast rate tensile tests. When strain aging embrittlement can occur in conjunction with these other types of embrittlement, the effects of hydrogen on the mechanical properties may be quite complex.

XI. SUMMARY

Hydrogen contamination can cause more than one type of embrittlement in alpha-beta titanium alloys. In this report attention is focussed upon strain aging embrittlement which occurs at room temperature. Only alpha-beta alloys are considered.

Strain aging embrittlement has its greatest effect on properties measured at slow strain rates. It can cause low ductility in room temperature tensile tests, and premature brittle fracture in room temperature rupture tests. The presence of stress concentrations lowers the applied load at which premature brittle fracture can occur.

Confidential

Susceptibility to strain aging embrittlement is a function of alloy composition and microstructure. Both the minimum hydrogen content required to produce embrittlement, and how slow the strain rate must be for embrittlement to be perceptible may be affected.

Strain aging embrittlement can occur whether or not the alloy composition is such that a eutectoid reaction is possible.

Examination of fracture surfaces suggests that premature brittle fracture consists of propagation of a crack until the residual cross-sectional area can no longer support the applied load, followed by ductile fracture in this residual cross-section.

In many of the alpha-beta alloys tested, metallographic examination of hydrogen contaminated specimens shows no evidence for a third phase either before or after fracture. In at least one alloy a third phase was visible after fracture.

Many of the broken ends of hydrogen contaminated mechanical property test specimens develop cracks which are parallel to the long axis of the specimen. This occurs after the specimen is broken in a mechanical property test which causes a triaxial state of stress. These cracks are presumably hydrogen embrittlement fractures due to residual radial stresses, and they tend to be intergranular.

Increasing test temperature seems to decrease the tendency towards hydrogen embrittlement but increase the rate at which it can occur.

A mechanism of strain aging embrittlement is suggested which involves microsegregation of hydrogen to the grain boundaries in plastically deformed material. This microsegregation involves diffusion of the hydrogen and proceeds at a finite rate. Properties measured in a mechanical property test depend upon whether the rate of deformation is fast or slow relative to the rate of microsegregation and consequent embrittlement.

1. Jaffee, R. I. and Campbell, I. E., "The Effect of Oxygen, Nitrogen and Hydrogen on Iodide Refined Titanium" Trans. AIME, 185, 646-655 (1949); Journal of Metals (September 1949).
2. Craighead, C. M., Lenning, G. A. and Jaffee, R. I. "Nature of the Line Markings in Titanium and Titanium Alloys" Trans. AIME, 194, 1317-1319 (1952); Journal of Metals (December 1952).
3. Lenning, G. A., Craighead, C. M. and Jaffee, R. I. "Constitution and Mechanical Properties of Titanium Hydrogen Alloys" Trans. AIME, 200, 367-376 (1954); Journal of Metals (March 1954).
4. Holden, F. C., Ogden, H. R. and Jaffee, R. I., "Heat Treatment, Structure and Mechanical Properties of Ti-Mn Alloys" Trans. AIME, 200, 169-184 (1954); Journal of Metals (February 1954).
5. Kotfila, R. J., and Erbin, E. F. "Hydrogen Embrittlement of a Titanium Alloy" Metal Progress 66, 128-131 (October 1954).
6. Burte, H. M., Erbin, E. F., Hahn, G. T., Kotfila, R. J., Seeger, J. W. and Wruck, D. A., "Hydrogen Embrittlement of Titanium Alloys" Metal Progress 67, 115-120 (May 1955).
7. Jaffee, R. I., Lenning, G. A. and Craighead, C. M. "The Effect of Testing Variables on the Hydrogen Embrittlement of Titanium and a Ti-8Mn Alloy" Paper presented at AIME meeting, N. Y., N. Y. (February 1956).
8. Craighead, C. M., Lenning, G. A. and Jaffee, R. I., "Hydrogen Embrittlement of Beta-Stabilized Titanium Alloys" Paper presented at AIME meeting, N. Y., N. Y. (February 1956).
9. Ripling, E. J. "Hydrogen Embrittlement of a Commercial Alpha-Beta Titanium Alloy" Trans. AIME, 206, 502-503 (1956); Journal of Metals (May 1956).
10. Kessler, H. A., Sherman, R. G. and Sullivan, J. F. "Hydrogen Affects Critical Properties in Commercial Titanium" Journal of Metals, 7, 242-246 (February 1955).
11. Slaughter, E. R. "Review of The Effects of Hydrogen in Steel" Journal of Metals, 8, 430-431 (April 1956).
12. Brown, J. T. and Baldwin, W. M. "Hydrogen Embrittlement of Steel" Trans. AIME, 200, 298-303 (1954).

Contrails

13. Zapflee, C. A. and Sims, C. E., "Hydrogen Embrittlement, Internal Stress and Defects in Steel" Trans. AIME, 145, 225-271 (1941).
14. Petch, N. J. and Stables, P. "Delayed Fracture of Metals Under Static Load" Nature, 169, 842-843 (1952).
15. Phillips, C. W. "The Effect of Heat Treatment on the Structure of a Commercial Titanium-Rich Alloy" Ph.D. Thesis, University of Michigan (1954).

TABLE I
ANALYSES OF TITANIUM ALLOYS
As Received Analysis (1)

Alloy	Heat	Al	Fe	Cr	Mo	Mn	C	N	O	H (ppm)
Ti-140A	M1170		2.1	2.5	1.6		0.09	0.03	0.13	250
C-130AM	B5038	3.2				3.2	0.04	0.05	0.15	60
C130AM	B3371	3.0				2.8	0.03	0.05	0.08	60
Ti-150A	R68		1.2	3.0			0.10	0.09	0.28	250
Ti-140A	M1192		2.0	2.2	1.7		0.09	0.02	0.10	210
Ti-155AX	Unknown	5.1	1.3	1.3	1.0		0.04	0.03	0.13	260

(1) Balance Titanium

TABLE II

PREPARATORY TREATMENTS TO ADJUST
HYDROGEN CONTENT AND THERMAL HISTORY

Alloy and Heat	As-received hydrogen level (ppm)	Hydrogen level tested (ppm)	Treatment applied to the as-received material
Ti-140A Ht. M1170	250	20	Vacuum anneal, 1200°F, 24 hrs. + furnace cool
		170	Vacuum anneal, 1200°F, 2 hrs. + air cool + heat in argon, 1200°F, 22 hrs. + furnace cool
		250	Heat in helium, 1200°F, 24 hrs. + furnace cool.
RC-130B Ht. B5038	60	10	Vacuum anneal, 1300°F, 25 hrs. + furnace cool
		320	Hydrogenate, 1300°F, 21 hrs. + air cool + heat in air, 1300°F, 4 hrs. + furnace cool
RC-130B Ht. B3371	60	60	Heat in air, 1300°F, 3 hrs. + furnace cool
		150	Hydrogenate, 1300°F, 21 hrs. + air cool + heat in helium, 1300°F, 5 hrs. + furnace cool.
		190	Hydrogenate, 1300°F, 21 hrs. + air cool + heat in helium, 1300°F, 5 hrs. + furnace cool
		280	Hydrogenate, 1300°F, 21 hrs. + air cool + heat in helium, 1300°F, 5 hrs. + furnace cool
Ti-150A Ht. R68	250	10	Vacuum anneal, 1300°F, 25 hrs. + furnace cool
		250	Heat in air, 1300°F, 24 hrs. + furnace cool.
Ti-140A Ht. M1192	210	210	Heat in air 1200°F, 24 hrs. + furnace cool
		210	Heat in air 1200°F, 24 hrs. + furnace cool + heat in air 1350°F, 22 hrs. + air cool.

TABLE II (cont'd)

PREPARATORY TREATMENTS TO ADJUST
HYDROGEN CONTENT AND THERMAL HISTORY

Alloy and Heat	As-received hydrogen level (ppm)	Hydrogen level tested (ppm)	Treatment applied to the as-received material
Ti-155AX	260	5	Heat in air, 1250°F, 0.5 hrs. + furnace cool + vacuum anneal, 1300°F, 24 hrs. + furnace cool.
		260	Heat in air, 1250°F, 0.5 hrs. + furnace cool + thermal treat in air, 1300°F, 24 hrs. + furnace cool.

TABLE III

THE EFFECTS OF HYDROGEN CONTAMINATION ON THE ROOM TEMPERATURE TENSILE
AND RUPTURE BEHAVIOR OF C-130AM, Ht. B5038. UNNOTCHED SPECIMENS

Hydrogen = 10 ppm

Hydrogen = 320 ppm

Tensile Tests

Test Speed	Time to Fracture (hr.)	0.2% Yield Strength (1000 psi)	Ultimate Tensile Strength (1000 psi)	Elong. in 4D (%)	Reduction in Area (%)
Fast	0.03	131	143	18	46
Slow	0.17	N.M.	138	20	43

Test Speed	Time to Fracture (hr.)	0.2% Yield Strength (1000 psi)	Ultimate Tensile Strength (1000 psi)	Elong. in 4D (%)	Reduction in Area (%)
Fast	0.03	126	145	17	39
Slow	0.17	N.M.	146	17	37
Very Slow	1.8	127	149	10	17

Rupture Tests

Stress (1000 psi)	Time to Fracture (hr.)	Reduction in Area (%)
137	2.3	46
135	27	40
133	62	43
129	Did not fracture in 1200 hrs.	

Stress (1000 psi)	Time to Fracture (hr.)	Reduction in Area (%)
144	0.04	33
143	1.3	12
136	9.0	9
129	22	5
123	442	3

TABLE IV

THE EFFECTS OF HYDROGEN CONTAMINATION ON THE ROOM TEMPERATURE RUPTURE BEHAVIOR OF T1-140A, Ht. MLI70. UNNOTCHED SPECIMENS

<u>Hydrogen = 10 ppm</u>			<u>Hydrogen = 170 ppm</u>			<u>Hydrogen = 250 ppm</u>		
Stress (1000 psi)	Fracture Time (hr.)	Reduction in Area (%)	Stress (1000 psi)	Fracture Time (hr.)	Reduction in Area (%)	Stress (1000 psi)	Fracture Time (hr.)	Reduction in Area (%)
137	0.4	52	136	0.3	16	138	0.1	19
118	Did not fracture in 803 hr.	.	131	13.1	13	119	2.4	3
102	Did not fracture in 1244 hr.	.	129	2.5	13	101	Did not fracture in 1244 hr.	

THE EFFECTS OF SPECIMEN SURFACE CONDITION
ON THE ROOM TEMPERATURE TENSILE BEHAVIOR
OF LOW HYDROGEN MATERIAL

<u>Surface Condition</u>	<u>Testing Speed (in./min.)</u>	<u>Ultimate Tensile Strength (1000 psi)</u>	<u>Reduction in Area (%)</u>
	C-130AM, Ht. B5038, 10 ppm		
Rough Polished	0.02	138	43
Fine Polished	0.02	142	44
	Ti-150A, Ht. R68, 10 ppm		
As Machined	0.1	142	52
Fine Polished	0.1	143	49
As Machined	0.02	143	52
Fine Polished	0.02	141	46

Contrails

TABLE VI

THE EFFECTS OF SPECIMEN SURFACE CONDITION
ON THE ROOM TEMPERATURE RUPTURE BEHAVIOR
OF C-130AM, Ht. B5038

<u>Surface Condition</u>	<u>Stress (1000 psi)</u>	<u>Time to Fracture (hr.)</u>	<u>Reduction in Area (%)</u>
		<u>10 ppm</u>	
Rough Polished	135	27	40
Fine Polished	135	9.3	39
		<u>320 ppm</u>	
As Machined	130	6.0	8.1
As Machined	130	6.7	9.4
Fine Polished	130	203	9.1
Fine Polished	130	47	10.6

THE EFFECT OF HEAT TREATMENT ON SUSCEPTIBILITY TO
HYDROGEN EMBRITTLEMENT. ROOM TEMPERATURE RUPTURE
TESTS ON NOTCHED SPECIMENS OF T1-140A, Ht. M1192

<u>Heat Treated Condition</u>	<u>Stress (1000 psi)</u>	<u>Time to Fracture (hr.)</u>
Furnace cooled	168	1.0
from 1200°F	146	4.0
Air cooled from	169	Did not fracture in 93 hr.
1350°F	143	Did not fracture in 1300 hr.

TABLE VIII

ROOM TEMPERATURE MECHANICAL PROPERTIES OF A MATERIAL WHICH DOES NOT EXHIBIT STRAIN AGING EMBRITTLMENT AT A HYDROGEN CONTENT OF 260 ppm. Ti-155AX.

HYDROGEN = 5 ppm

HYDROGEN = 260 ppm

Tensile Tests

Testing Speed (in./min.)	Unnotched Ultimate Tensile Strength (1000 psi)	Unnotched Reduction in Area (%)	Notch Tensile Strength (1000 psi)	Testing Speed (in./min.)	Unnotched Ultimate Tensile Strength (1000 psi)	Unnotched Reduction in Area (%)	Notch Tensile Strength (1000 psi)
0.1	159	44	-	0.1	165	40	-
0.02	161	45	253	0.02	164	37	252

Unnotch Rupture

Stress (1000 psi)	Time to Fracture (hr.)	Reduction in Area (%)	Stress (1000 psi)	Time to Fracture (hr.)	Reduction in Area (%)
158	1.2	4.3	157	106	4.3
154	Did not fracture in 1200 hrs.		156	Did not fracture in 1200 hrs.	

Notch Rupture

Stress (1000 psi)	Time to Fracture (hr.)	Stress (1000 psi)	Time to Fracture (hr.)
200	64	200	122
176	Did not fracture in 650 hrs.	176	Did not fracture in 652 hrs.

Control

● SLOW (0.02 IN./MIN.)

○ FAST (0.1 IN./MIN.)

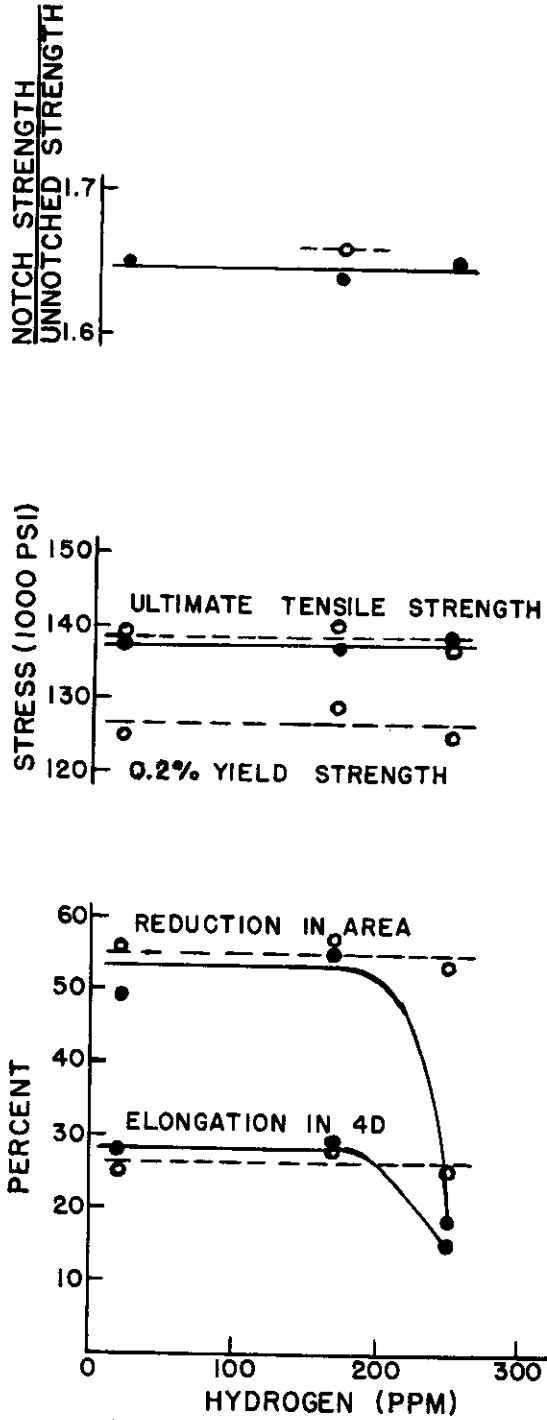


Figure 1. The Effects of Hydrogen on the Room Temperature Tensile Properties of Ti-140A, Ht. M1170. Unnotched Specimens Except Where Indicated.

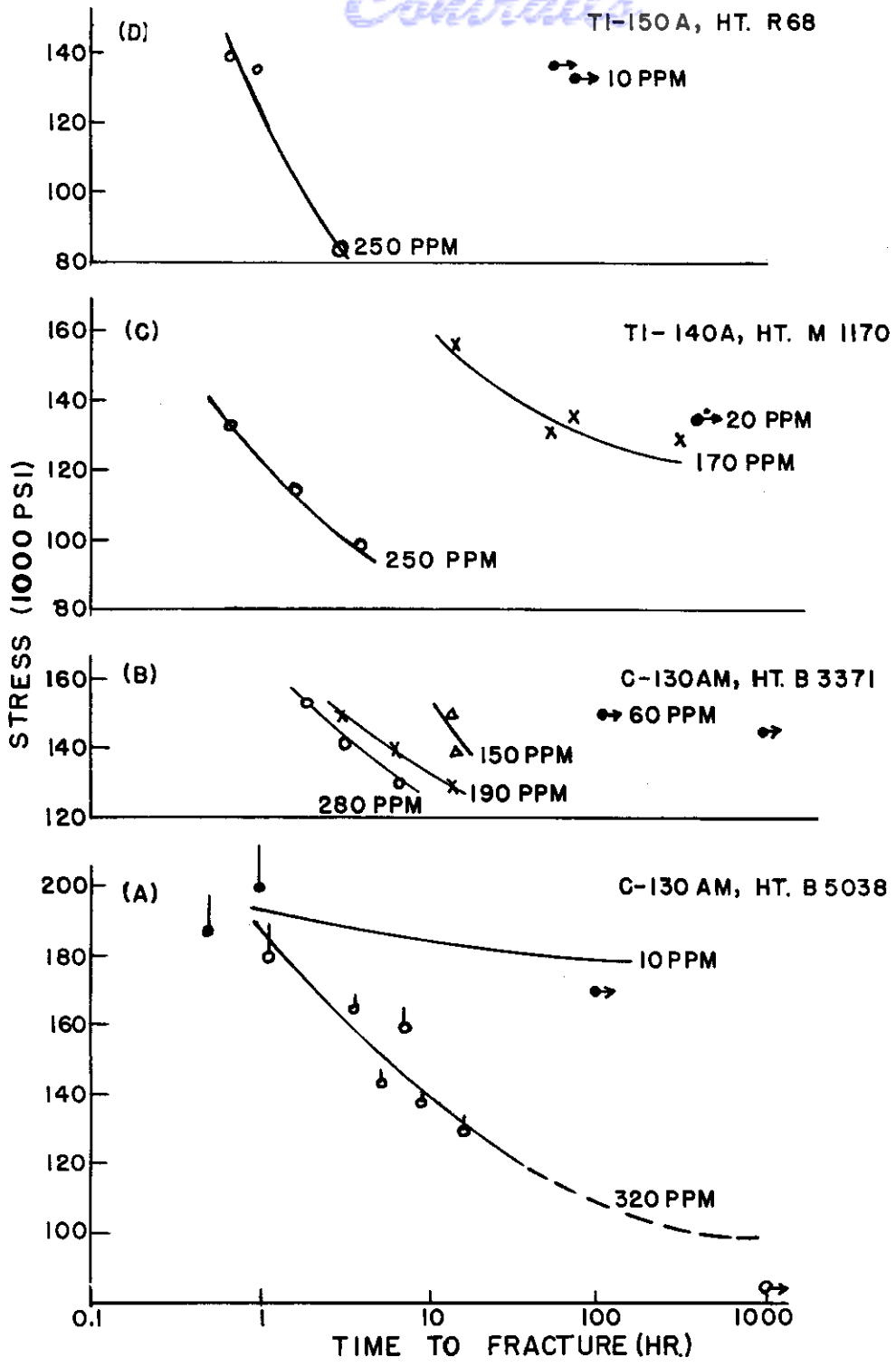


Figure 2. The Effects of Hydrogen on the Room Temperature Rupture Behavior of Notched Specimens. In (A) the Height of a Line Extending Above a Point is Proportional to the Reduction in Area at Fracture.

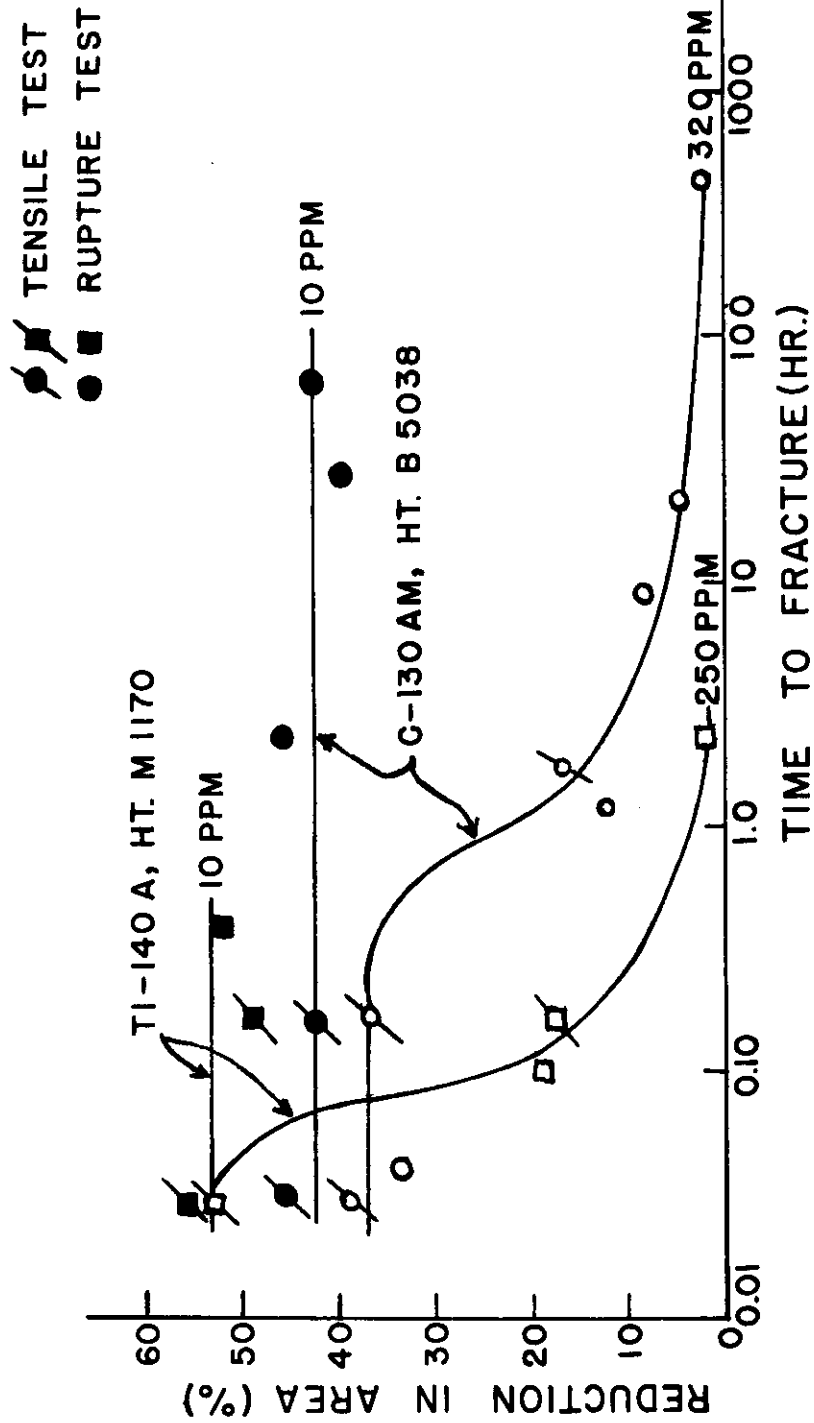
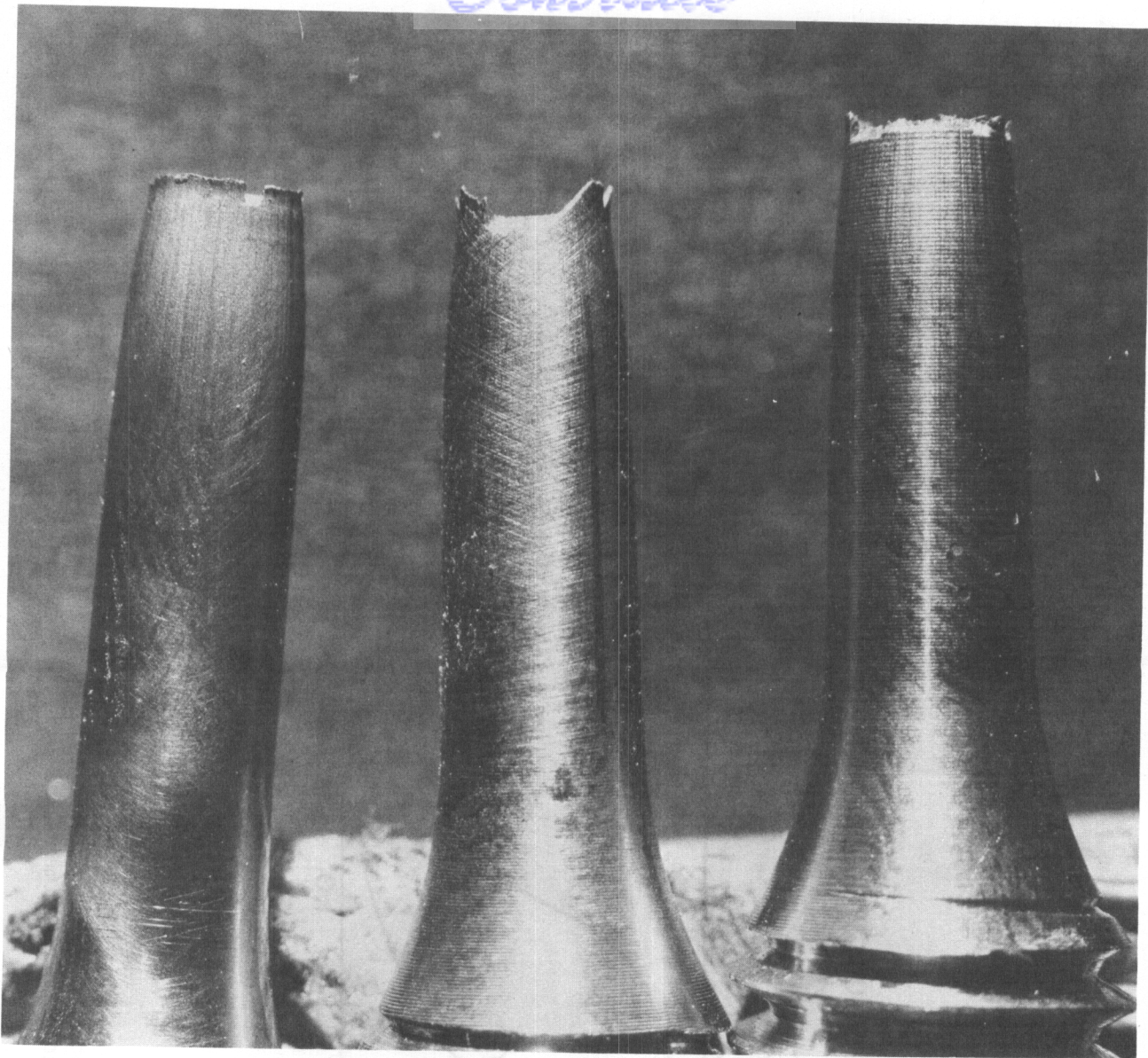


Figure 3. The Influence of Time to Fracture on Ductility Measured in Room Temperature Tensile and Rupture Tests. Unnotched Specimens.

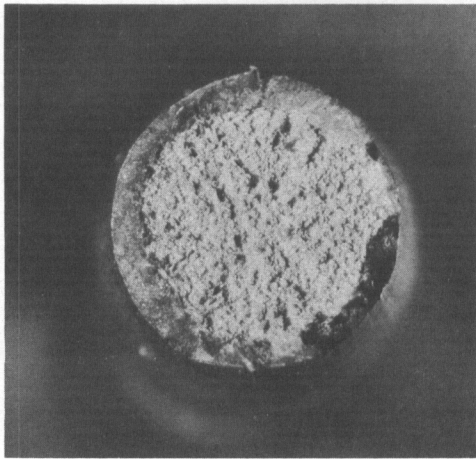


a. Fine Polished

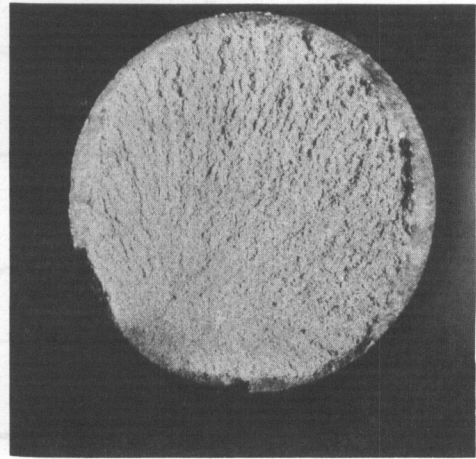
b. Rough Polished

c. As Machined

Figure 4. The Effects of Specimen Surface Condition



a. Ductile Fracture



b. Brittle Fracture Due to Strain Aging Hydrogen Embrittlement

Figure 5. The Appearances of Fracture Surfaces for Unnotched Specimens.

Contrails

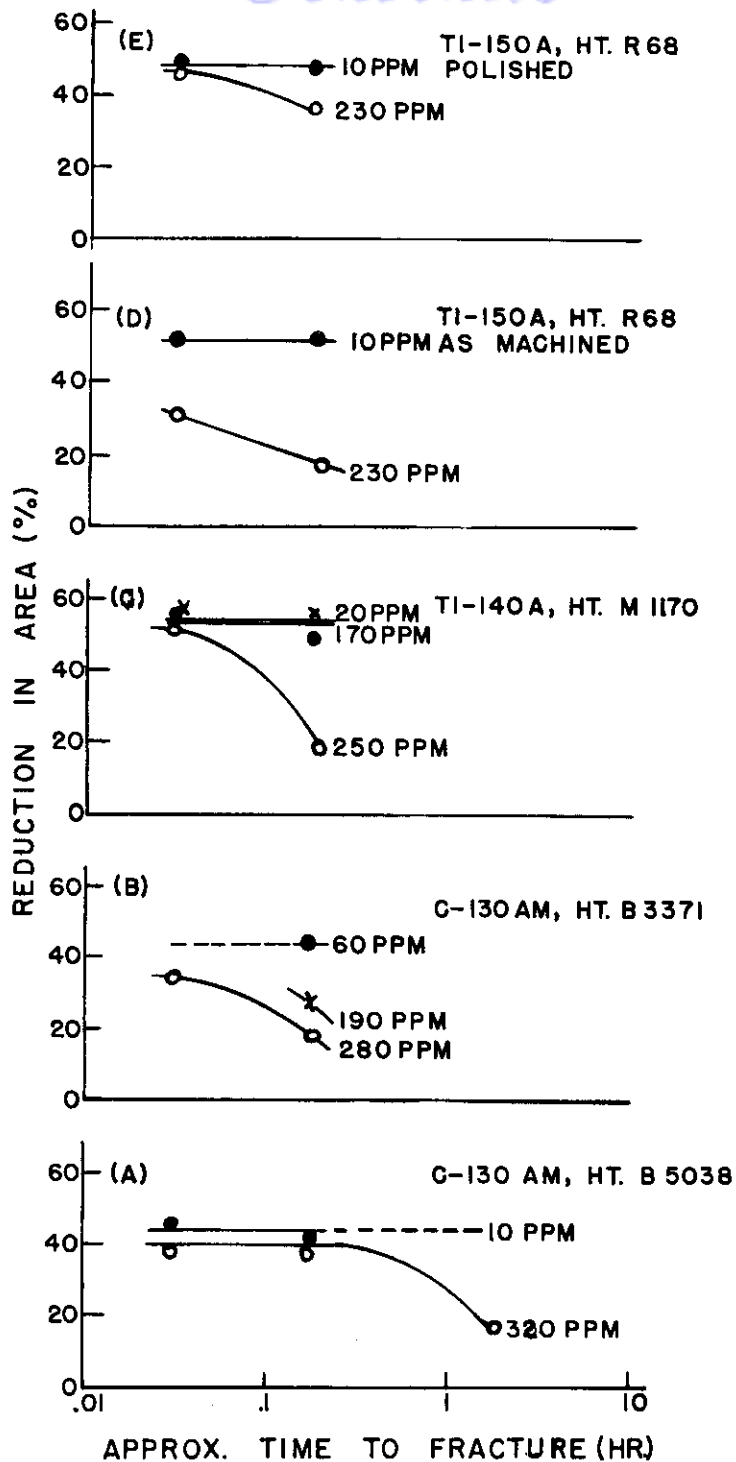
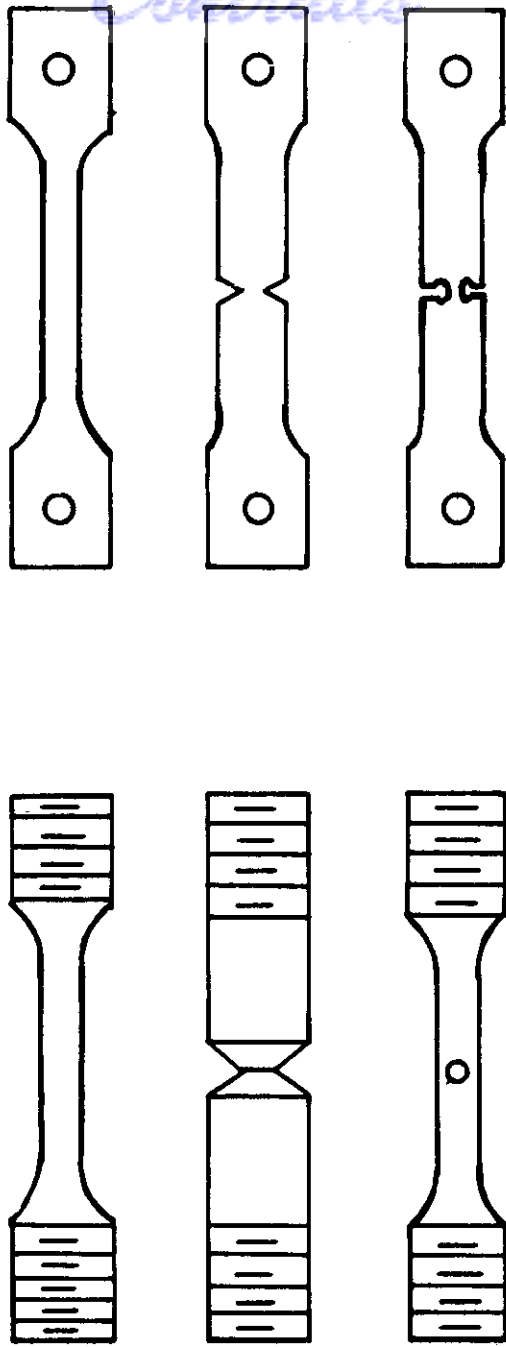


Figure 6. The Effects of Various Factors on Ductility Measured in Room Temperature Tensile Tests. Unnotched Specimens.

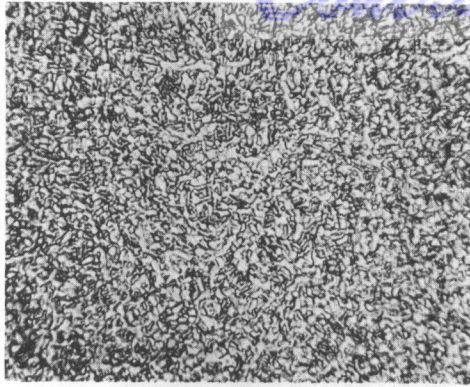


SHEET SPECIMENS

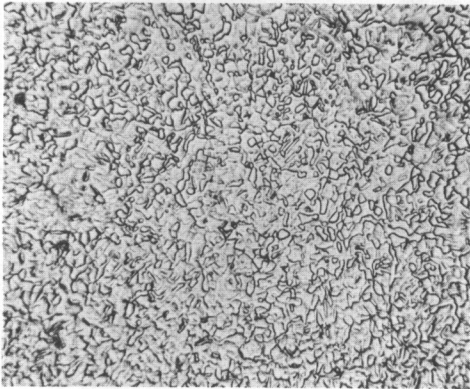
CYLINDRICAL SPECIMENS

Figure 7. Mechanical Property Specimens that have been Tested. Not Drawn to Scale. Mechanical Property Data are Reported Only for the Unnotched and V-Notched Cylindrical Specimens.

Contrails

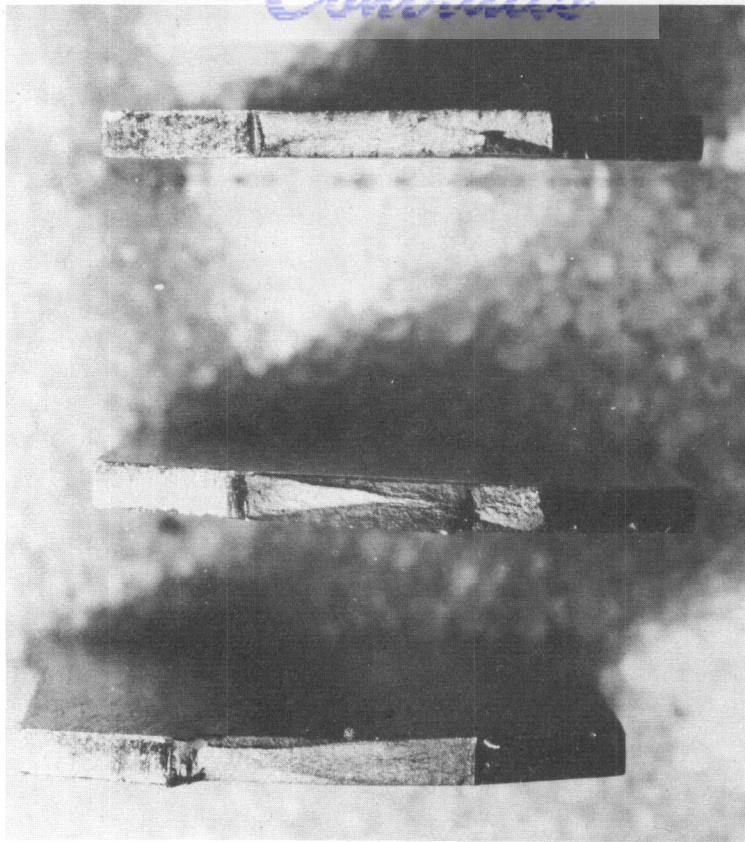


a. Furnace Cooled From
1200°F



b. Air Cooled From
1350°F

Figure 9. Photomicrographs of Ti-140A, Ht. M1192, 210 ppm
Unstrained Material. Perpendicular to Rolling
Direction. Mag. 500X.



a.

b.

c.

Figure 10. The Appearances of Fractures in Notched Specimens of Ti-6Al-4V Sheet.

- a. Ductile Fracture. Hydrogen = 50 ppm, Short Time Tensile Test.
- b. Brittle Fracture. Hydrogen = 800 ppm, Rupture Test at 130,000 psi, Rupture Time = 9 hrs.
- c. Brittle Fracture. Hydrogen = 800 ppm, Rupture Test at 60,000 psi, Rupture Time = 91 hrs.

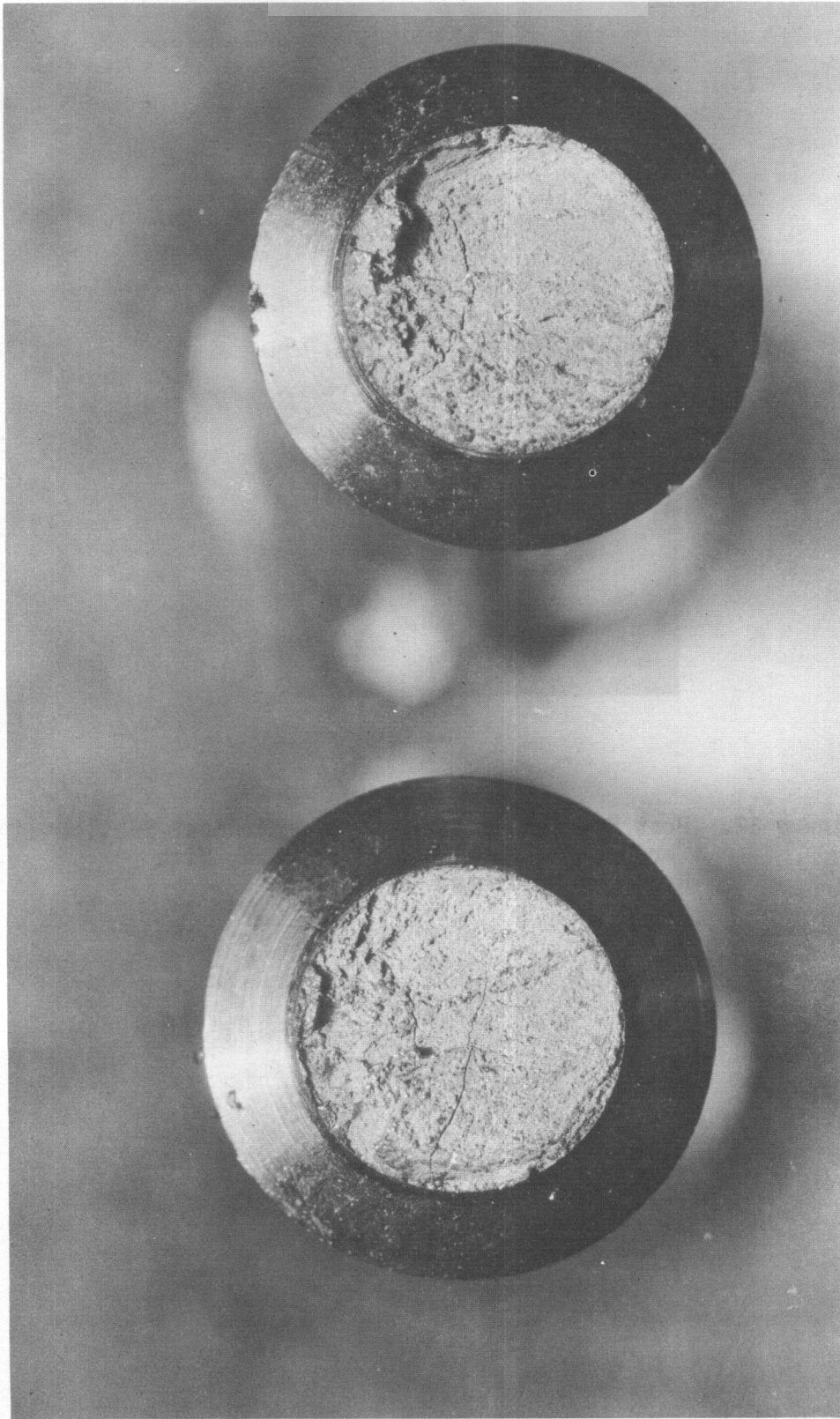


Figure 11. The Appearance of the Fracture Surface for Notched Specimens of High Hydrogen Material. Both Ends of One Specimen. Note the Post Fracture Cracks.

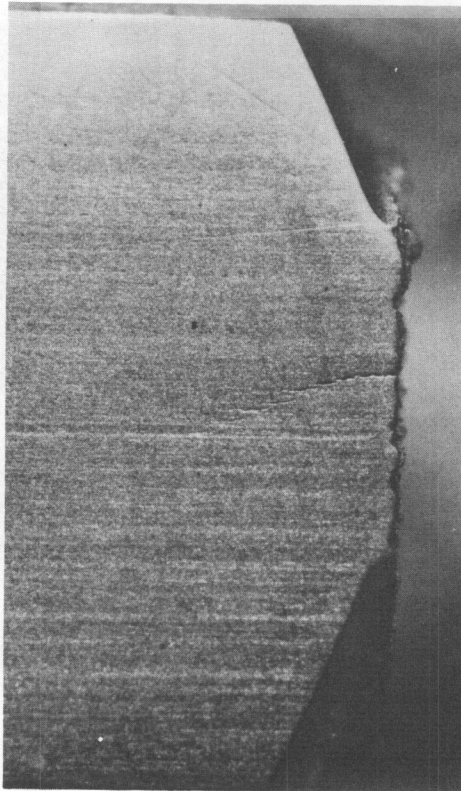
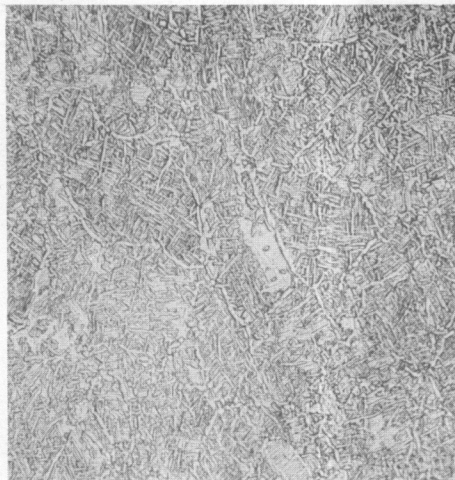


Figure 12. Post Fracture Cracking. Longitudinal Section Through Fractured End of Notched, High Hydrogen Specimen.

a. 20 ppm



b. 170 ppm

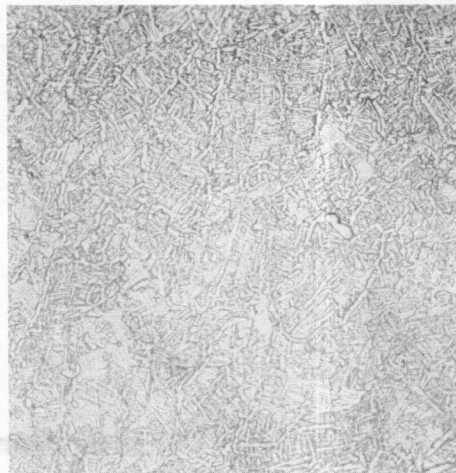
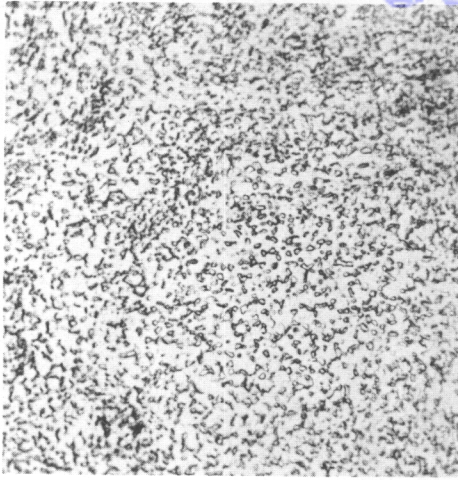
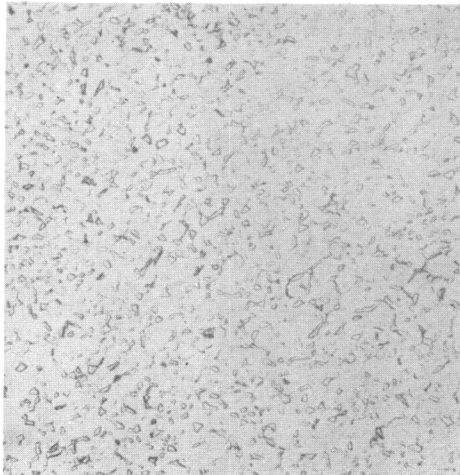


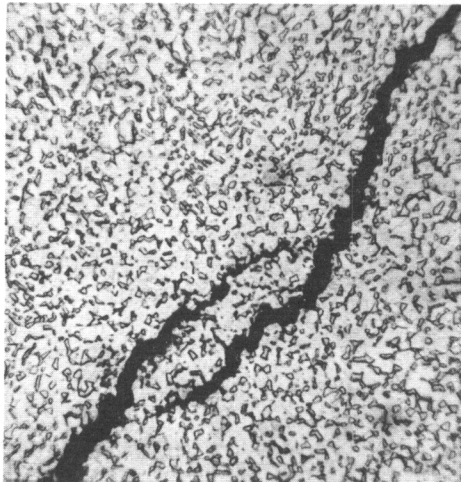
Figure 13. Photomicrographs of Ti-140A, Ht. M170. Unstrained Material. Perpendicular to Rolling Direction. Mag. 500X.



a. 60 ppm, Near Fracture



b. 280 ppm, Unstrained Material



c. 280 ppm, Near Fracture

Figure 14. Photomicrographs of C-130AM, Ht. B3371. Perpendicular to Rolling Direction. Mag. 500X.

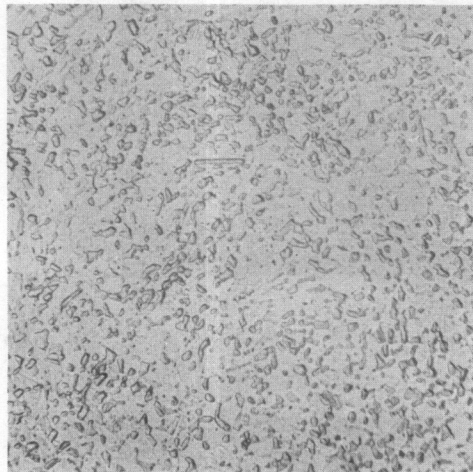
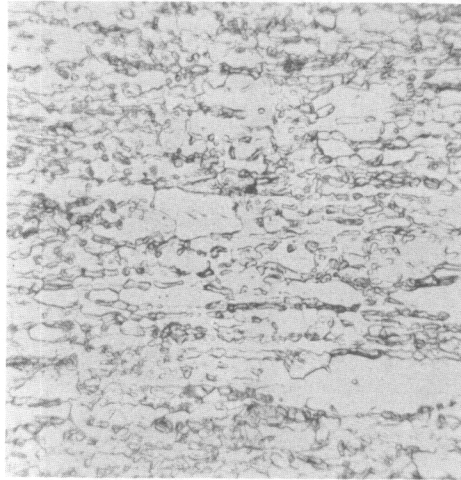


Figure 15. Photomicrograph of C-130AM, Ht. B5038, 320 ppm. Unstrained Material. Perpendicular to Rolling Direction. Mag. 500X.

a. Unstrained Material



b. Near Fracture

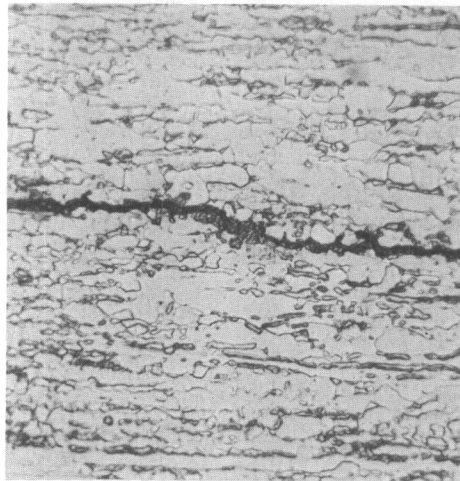
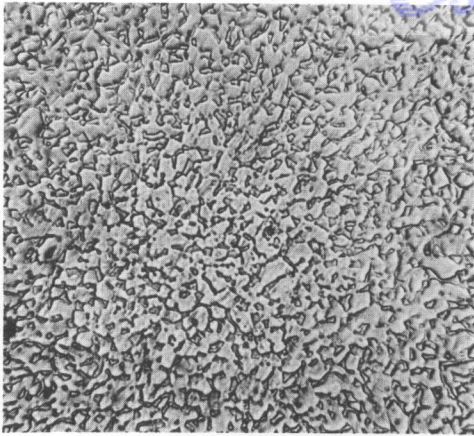
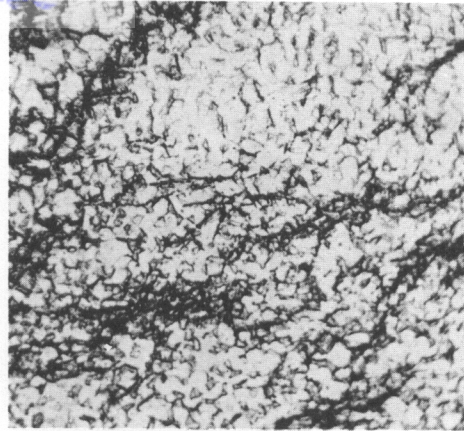


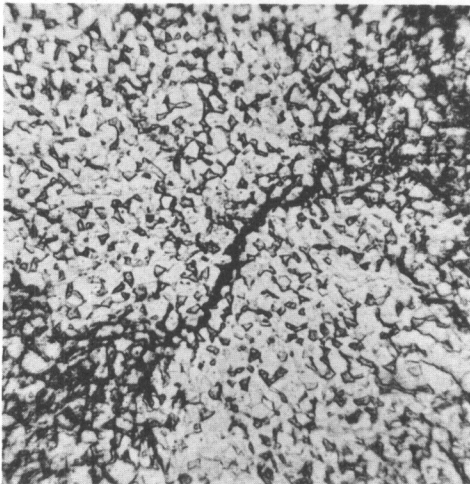
Figure 16. Photomicrographs of C-130AM, Ht. B5038, 320 ppm.
Parallel to Rolling Direction. Mag. 500X.



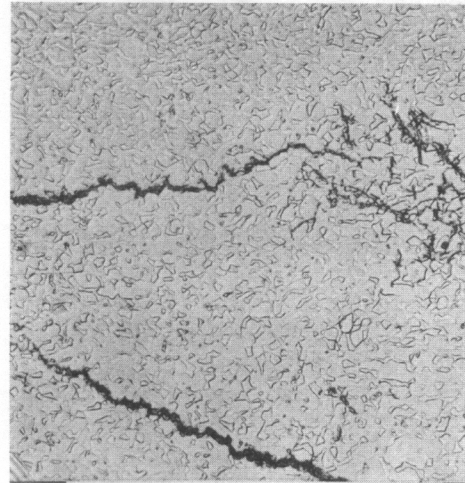
a. Unstrained Material



b. Near Fracture. Third Phase

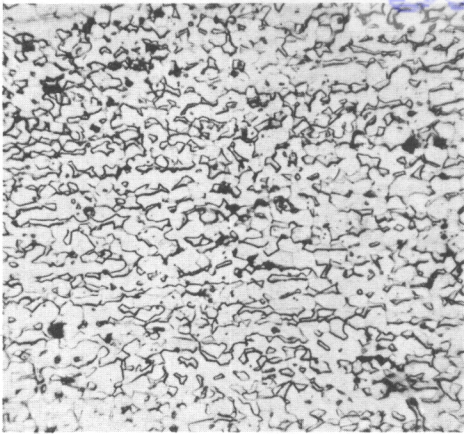


c. Near Fracture. Post Fracture Crack and Third Phase

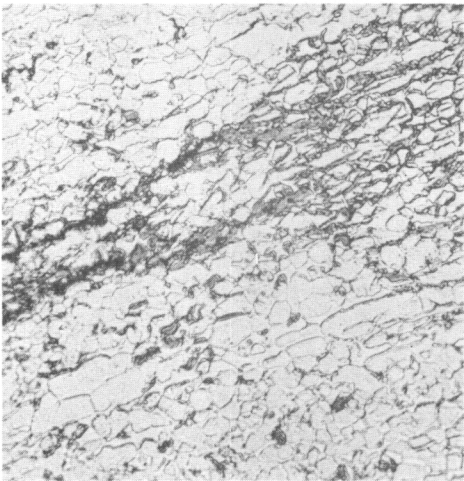


d. Post Fracture Crack Plus Partially Redissolved Third Phase

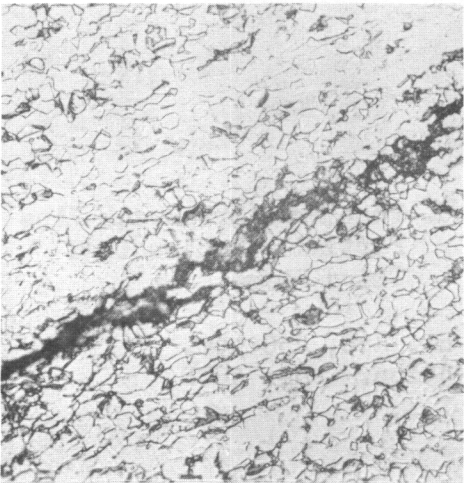
Figure 17. Photomicrographs of Ti-150A, Ht. R68, 250 ppm. Perpendicular to Rolling Direction. Mag. 500X.



a. Unstrained Material



b. Near Fracture. Third Phase at End of Post Fracture Crack.



c. Near Fracture. Post Fracture Crack

Figure 18. Photomicrographs of Ti-150A, Ht. R68, 250 ppm.
Parallel to Rolling Direction. Mag. 500X.

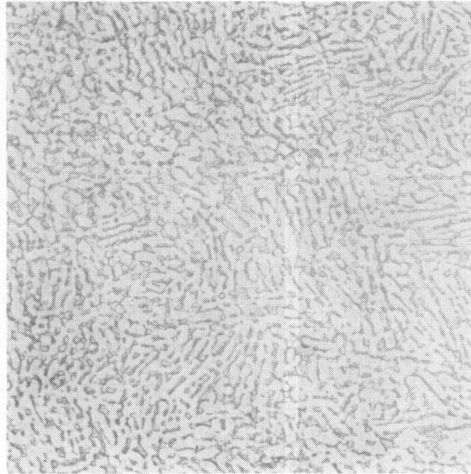


Figure 19. Photomicrograph of Ti-155AX, 260 ppm. Unstrained Material. Perpendicular to Rolling Direction. Mag. 500X. This Material not Susceptible to Strain Aging Hydrogen Embrittlement.